

High Temperature Superconductivity in the Cuprates: Phenomena from a Theorist's Point of View

T V Ramakrishnan

Indian Institute of Science, Bangalore and JNCASR, Jakkur, Bangalore

Abstract. I present a selection of experimental results on metallic cuprates, both above the superconducting transition temperature T_c (often called the strange metal state) and in the superconducting state. It highlights this still poorly understood part of the physical world. After an introduction, I talk briefly about the pseudogap regime and about the unusual linear resistivity phenomenon. Several empirical correlations between observed quantities are mentioned, e.g. T_c and superfluid density (Uemura), T_c and next nearest neighbour hopping, slope of the linear resistivity and T_c . In the belief that a comprehensive explanation may need an understanding of the extremely strongly correlated metal, a few initial steps in this direction are outlined.

1. Introduction

It is a great honour to participate in a meeting marking a hundred years of the revolutionary work of Satyendranath Bose. Bose's pioneering work on an ideal gas of photons showed us how to count states of a collection of identical, free, massless, spinful, quantum particles. It marked a turning point; quantum statistical physics was born. For this reason, the great theoretical physicist Landau regarded him as one of the founders of quantum physics along with Bohr, Heisenberg, Schroedinger and Dirac.‡

As is well known, Einstein applied the quantum statistics of Bose [1] to particles with nonzero rest mass. He showed that below a certain temperature, inevitably, a macroscopic fraction of them condenses into a single quantum state [2]; this is Bose (or Bose Einstein) condensation. Very soon after the discovery of superfluidity in Helium (1937), London identified superfluidity with Bose condensation [3]. Later, he argued that superconductivity is due to macroscopic quantum coherence, a phenomenon akin to Bose condensation [4, 5]. On the face of it, macroscopic quantum coherence in a metal appears unlikely; the constituent electrons are subject to the Pauli exclusion principle so that no two of them can be in a single quantum state, let alone a very large number being in the same state. Their binding into pairs (Cooper pairs) which are Bose like objects and the description of a superconductor as a phase coherent collection of these Cooper pairs is the celebrated Bardeen, Cooper and Schrieffer (BCS) theory of superconductivity [6], proposed in 1957. It seems even more improbable that cuprates could be superconducting, since additionally, electrons in them repel each other strongly and locally (strong electron correlation, indicated by large positive U in the Hubbard model) [7]. However, very soon after the discovery of high temperature superconductivity in the cuprates [8] in 1986, Anderson [9] argued that superconductivity can occur in purely and strongly repulsive electron systems, and proposed a mechanism (resonating valence bond or RVB) for it.

Two unexpected discoveries in the physics of quantum matter dating to the 1980s, namely the

‡ Landau had a logarithmic 'genius scale' for physicists, ranging from 0 to 5. Newton was at 0 on this scale and Einstein was at 0.5. Bose, along with foundational figures of quantum physics like Bohr, Schrodinger, Heisenberg, Dirac... was at 1. Landau put himself at 2.5, and was finally promoted to 2.

quantum Hall effect [10] and high temperature superconductivity in the cuprates [8] have given birth to new directions in condensed matter physics. The recognition of topology as a widely prevalent and robust feature of condensed matter systems with unexpected consequences flowed from the former. The basic electronic nature of the latter, namely of the cuprates and their superconductivity, is still a relatively unsettled question while it is possible that the answer has the potential to open up a large domain of quantum matter for deeper exploration. Although cuprate phenomena (both in the nonsuperconducting or 'normal' metallic as well as in superconducting phases) no longer occupy center stage in the field of condensed matter physics, a huge mountain of work has accumulated (there are apparently more than 2,00,000 papers on the subject) and surprising major effects continue to be discovered. There has been great progress both theoretically and experimentally in the field. There are many demanding and highly sophisticated theoretical approaches. However, the broad view seems to be that we do not quite understand the unusual goings on in them as a whole.

In this article, I introduce the cuprate family in section 2 and describe some experimental features (Sections 3 to 5) limited by my knowledge, memory and understanding. Fortunately, there is a large review literature on the subject; synoptic reviews [11], detailed surveys of parts of the field e.g. ref. [?] and books (e.g. the one edited by Schrieffer and Brooks) [12]. Some of the data presented here are more recent. The correlations presented here are known, but are put together here in one place for the first time. They seem to call for a comprehensive and detailed theory in the strong correlation genre. High temperature superconductivity in the cuprates probably provides us with a glimpse of a Bose condensation like phenomenon which may require a basic departure in quantum physics.

2. Cuprates: the basics

Cuprates in which Cu occurs in the electronic configuration Cu^{++} § are a large family with more than 30 chemically distinct members. To model their electronic properties, we start with the 'mother

§ namely with a partially filled d shell having 9 rather than 10 d electrons, therefore necessarily with d electron states near the Fermi energy.

compound' La_2CuO_4 . La_2CuO_4 in which a fraction of the trivalent La atoms are replaced by divalent Ba was the first discovered high T_c superconductor [8]; in general high T_c superconductivity in this family results for systems for the doped systems $La_{2-x}Ae_xCuO_4$ where x is therefore the amount of hole doping (δ doping in the semiconductor language) and Ae is an alkaline earth. The most commonly used alkaline earth is Sr .

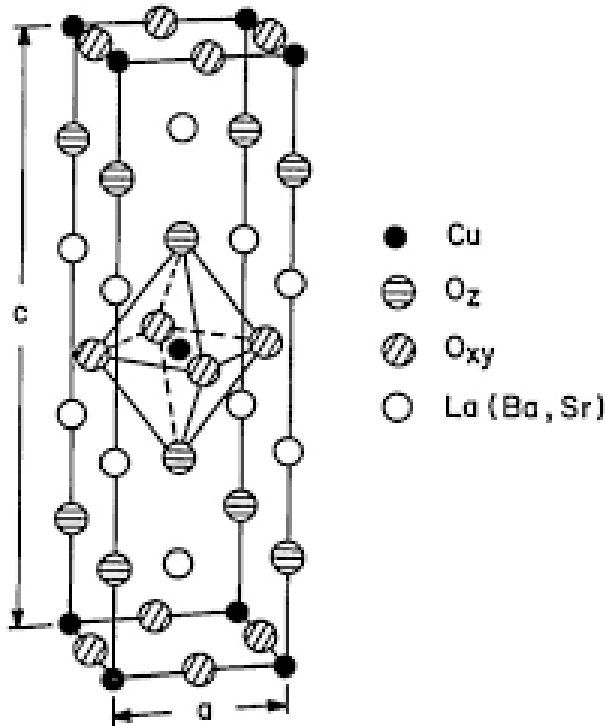


Figure 1. Schematic picture of a unit cell of stoichiometric La_2CuO_4 crystal.

The crystal structure of La_2CuO_4 is shown in Fig. 1. This can be thought of as an ‘enhanced’ perovskite; namely as ABO_3 (perovskite) + AO where $A \rightarrow La$ and $B \rightarrow Cu$. (This is one reason why the solid state chemists Ganguly and Rao were interested [13] in it around 1984, and showed that it is an antiferromagnetic Mott insulator). The perovskite is highly distorted; it is a ‘pointy’ octahedron with BO along the c axis or z direction being $\approx 2.46\text{\AA}$, and BO in ab or xy plane being $\approx 1.91\text{\AA}$. As a consequence, the system is accurately and most simply thought of as planar layers of $(Cu - O_2)$ (square plane with Cu at the corners of the square, and O atoms at the centre of the shortest $Cu - Cu$ line, namely the square edge) interspersed with $La - O$ layers.

This general feature is apparent from the schematic unit cell pictures of three well known cuprate

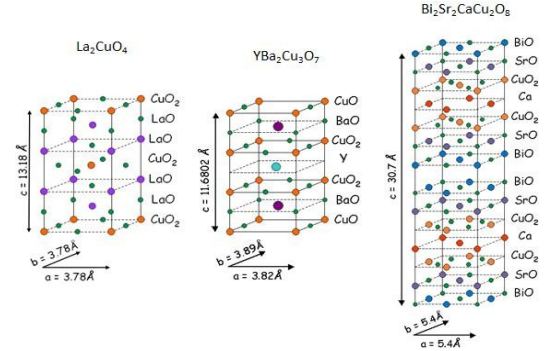


Figure 2. Unit cells of three common members of the cuprate family, namely La_2CuO_4 , $YBa_2Cu_3O_7$ and $Bi_2Sr_2CaCu_2O_8$.

types shown in Fig. 2, namely La_2CuO_4 (often called *LCO*; the compound doped with Sr is called *LSCO*), $YBa_2Cu_3O_7$ (called *YBCO*) and $Bi_2Sr_2CaCu_2O_8$ (called *Bi - 2212*). We see well separated layers of $(Cu - O_2)$ (e.g. the top and bottom and middle layers for *LCO* in Figs. 1 and 2; the bilayers in *YBCO* and *Bi - 2212* in Fig. 2). The hole doping in these is accomplished by substituting trivalent La with divalent Sr for example, and by oxygen deficiency (*YBCO*) or excess (*Bi - 2212*). In the latter two systems, greater oxygen deficiency corresponds to lower hole doping (*YBCO*) and larger oxygen excess to higher doping (*Bi - 2212*). The doping level x is generally estimated using the Presland [14] formula.

Fig. 3 (a) depicts the single site d orbital energy level for a free atom (tenfold degenerate), and for an atom in a perfect octahedral symmetry crystal field (which splits this into lower lying degenerate d_{yz} , d_{xz} , d_{xy} symmetry orbitals accommodating six electrons in all and higher lying $d_{3z^2-r^2}$, $d_{x^2-y^2}$ orbitals with a maximum of four electrons in them). It also shows that the Jahn Teller splitting of the perfect octahedral coordination (resulting in a ‘pointy’ octahedron) splits the degeneracy of the upper levels, with the ‘antibonding’ $d_{x^2-y^2}$ symmetry level being higher in energy. For nine electrons in the d shell, consequently there is one electron (or hole) in the (local) $d_{x^2-y^2}$ symmetry orbital. These are the electron and the state we focus on. Fig. 3 (b) shows schematically that (as in a stoichiometric cuprate) if there is exactly one d electron per site, electron transport requires that there will necessarily be two electrons on the site to which the electron hops. This costs an extra energy U . If this is large (larger than the kinetic energy gained by motion), such a real hopping does not take place, each electron stays put, and the system is an insulator, a Mott insulator. If there are

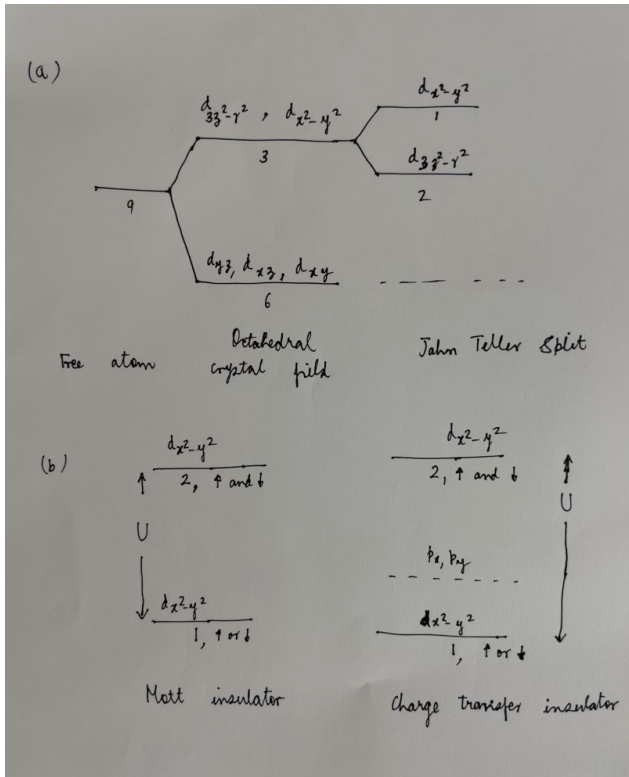


Figure 3. (a) d electron levels of Cu^{++} in a free atom, in a perfect octahedral environment, and in an octahedral environment with Jahn Teller splitting of the kind that occurs in the cuprates. Electron occupation is also indicated. (b) Mott and charge transfer insulators, shown schematically.

unoccupied p_x or p_y states within the Mott-Hubbard gap of energy $\approx U$ (as in the cuprates) the lowest energy excitation involves transferring an electron from a $d_{x^2-y^2}$ orbital to a p orbital and the system is a charge transfer insulator [15].

With this background, I model the interesting low electron excitation energy states of the cuprates by considering only the uncoupled parallel planes with side sharing square unit cells each with Cu atoms at corners and O atoms at centers of sides. There are $d_{x^2-y^2}$ local symmetry orbitals situated at Cu sites, p_x and p_y orbitals at O sites. Each orbital can accommodate two electrons. There is onsite electron repulsion between electrons in these orbitals; and one has intersite hopping. A very common description of hole doped cuprates is the following. The hole migrates to the p_x , p_y orbitals of the plane because of the strong coulomb attraction to the $(Cu - O_2)$ collection. Zhang and Rice [16] showed (see also ref. [17]) that it hybridizes with the local orbital of $d_{x^2-y^2}$ symmetry and forms a strongly bound spin singlet (or spinless) hole state. Therefore, the simplest picture which has a chance of being realistic is an effective one band Hubbard model (two d square lattice, $d_{x^2-y^2}$ local

symmetry orbital at site i) with such holes. This is described by the following Hamiltonian $(H - \mu N_e)$ in a grand canonical ensemble:

$$H - \mu N_e = \sum_{i,\sigma} (\varepsilon_d - \mu) a_{i\sigma}^\dagger a_{i\sigma} + \sum_{i,j} t_{ij} a_{i\sigma}^\dagger a_{j\sigma} + U \sum_i n_{i\uparrow} n_{i\downarrow} \quad (1)$$

All the other electronic states have been ‘integrated out’, and their effect appears in the parameters of this effective one band Hubbard model. It is perhaps the most commonly used model for describing the cuprates. Here, ε_d is the energy of the $d_{x^2-y^2}$ orbital at site i , the chemical potential μ is such that one has x holes or $(1 - x)$ electrons per site, t_{ij} is the hopping amplitude from site i to site j and U is the on site Mott-Hubbard repulsion. Very many experimental and theoretical efforts have provided estimates for the parameters of the Hamiltonian. A common one is: t (the nearest neighbour hopping amplitude) $\approx 0.4eV$, t' (the next nearest neighbour hopping amplitude) $\approx -0.3t$ and $U \approx 4 - 7eV$ (see e.g. ref [7] for a survey as well as a calculation of U).

An obvious question is: do we have a theory of superconductivity in the cuprates in this model? It is a measure of the fractious nature of the subject that there is no convergence on this issue. As mentioned above, there is an RVB mechanism of superconductivity proposed by Anderson [9] and developed by him and Baskaran [18] as well as a ‘plain vanilla’ strong correlation theory described by him and a number of collaborators [19]. On the other hand, we know a large number of specific properties of cuprate superconductors and of the strange metal from which the superconductivity arises; these have not yet found an explanation in the theory. In the next few sections (Sections 3 - 5) we detail experimental properties whose comprehensive and coherent explanation would constitute a complete theory.

We situate the description of experimental phenomena in the observed phase diagram of hole doped cuprate superconductors. An early, simplified, universal phase diagram in the hole density x temperature T plane, due to Norman [20] is shown in Fig. 4. (The hole concentration x in cuprates is mostly inferred from the highly successful empirical Presland [14] formula). The stoichiometric cuprate ($x = 0$) is a Néel antiferromagnetic insulator below T_N . The material is a paramagnetic insulator above T_N , a signature of the Mott or correlated insulator. The Néel order and the insulating phase disappear very rapidly with doping; typically, for $x > 0.04$ there

|| In the literature, x is often referred to as p , the symbol for a hole in semiconductor physics

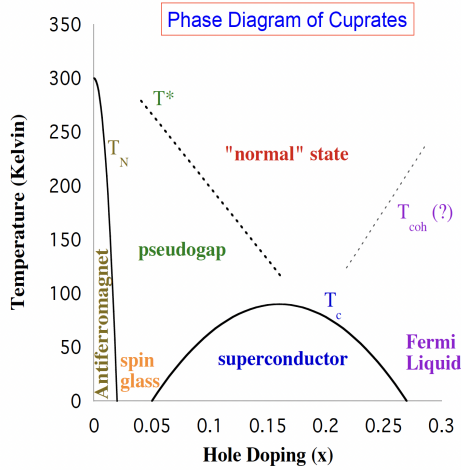


Figure 4. Phase diagram of the hole doped cuprates in the hole x (or p) and temperature T plane (from Norman, [20]).

is no Néel order. There is a very narrow regime of glassy insulating phase for larger x at low temperatures around this x . The superconducting phase begins at around $x \approx 0.04$ (say x_{min}) and continues till $x \approx 0.27$ (say x_{max}) in a roughly parabolic dome shaped curve in the (x, T) plane. T_c is maximum for about $x \approx 0.16$; this is generally called optimum doping x_{opt} . The system is called underdoped for $x < x_{opt}$ and overdoped for $x > x_{opt}$. Most of the early work concentrated on the underdoped regime. Recently, there is much more activity in the overdoped region. Beyond the doping $x = x_{max}$, the low temperature region is marked Fermi liquid, which is characterized for example by the imaginary part of the self energy $\Sigma(\omega, T)$ having a specific quadratic dependence on ω and on T . This Fermi liquid behaviour continues with increasing temperature and hole density till a dotted curve region marked T_{coh} with a question mark(?), above which the Fermi liquid becomes incoherent. For values of x less than x_{opt} , we have, above T_c , a region marked pseudogap below a temperature $T^*(x)$ with distinct properties some of which are mentioned below. Beyond the green dotted line where the pseudogap ends, there is a region marked ‘normal’ state. This roughly fan shaped region is seen to encompass the slightly underdoped as well as overdoped regimes of x . Their properties have been explored very actively in the last decade or so. The thermodynamic phases are two, namely the antiferromagnetically ordered one and the superconductor. Their boundaries are indicated by full lines. The other ‘phases’ are regions with different distinct characteristic behaviour crossing over smoothly. There is a controversy about whether the pseudogap is a distinct thermodynamic phase ending in a line of critical points separating the ‘normal’ state, or

whether it is a crossover regime (for example whether in the figure, T^* should be indicated by a dotted line or a full line).

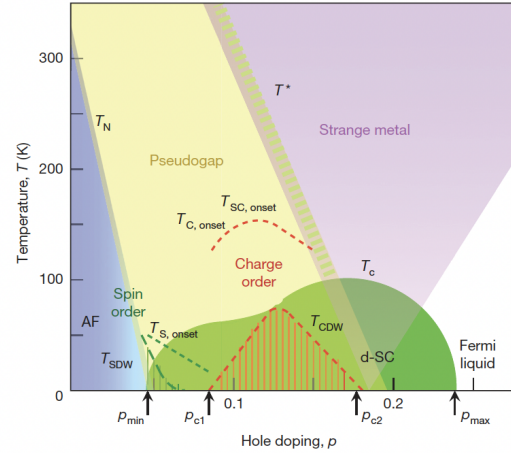


Figure 5. Phase diagram of the hole doped cuprates in the hole x (or p) and temperature T plane (from Keimer et al., [11]).

A somewhat more realistic and recent phase diagram [11] is shown in Fig. 5. The shape of the superconducting dome is close to what is actually seen in $La_{2-x}Sr_xCuO_4$. Many ordering tendencies, specially in the underdoped region, are indicated, e.g. spin order, charge (CDW) order. The ‘normal’ state is labelled as strange metal, which is the present nomenclature for it.

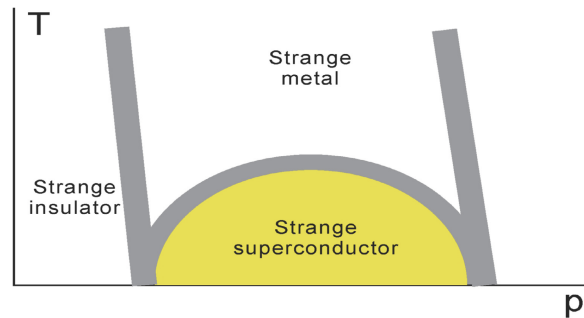


Figure 6. A caricature of the hole doped cuprate phase diagram, emphasizing its strangeness (from Bozovic, [21]).

In Fig. 6, I show a schematic version of the phase diagram, from an article [21] by I. Bozovic, an experimentalist who has done experiments on carefully MBE deposited LSCO samples from underdoped to overdoped with well defined x (or p), for decades. He argues here that all the three broad regimes in the hole doped cuprate phase diagram, namely the insulator, the metal, and the superconductor are strange. I now

describe some phenomena in two regions, namely the metal and the superconductor; we see that the properties are indeed unlike those of ‘conventional’ metals and superconductors. I focus on experimental results which can be obtained from the data without too much ‘processing, e.g. resistivity ρ and critical temperature T_c . I also emphasize correlations between two measured quantities.

3. The Pseudogap

The defining feature of this regime (which is in the underdoped hole density x regime above T_c and is bounded by the temperature $T^*(x)$) is the pseudogap observed in the single particle density of states.

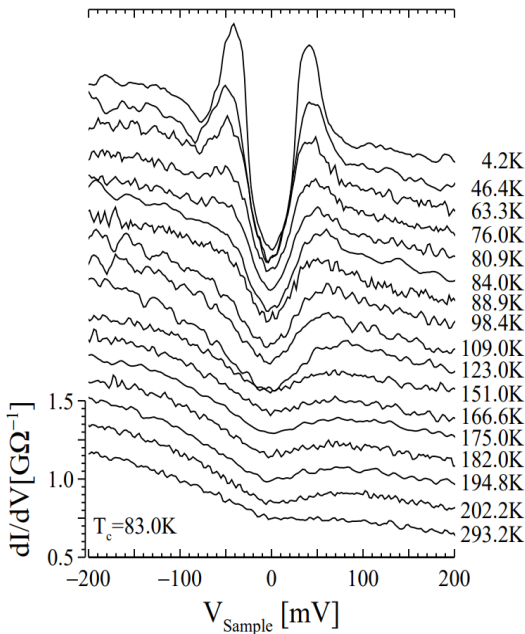


Figure 7. Pseudogap in the electron density of states (from Kordyuk, ref. [22]).

Fig. 7 (from a 2015 review by Kordyuk, ref. [22]) shows ARPES data for a sample of *Bi* – 2212 at different temperatures; the T_c is 83.0K. We notice a U shaped dip in the inferred density of states (DOS). It is centred around the Fermi energy and is most prominent at the lowest measurement temperature (4.2K) where it is almost a gap. (One can also see a clear particle hole asymmetry). As temperature increases, the dip becomes shallower. It does not vanish at T_c , where superconductivity disappears (as happens for the measured DOS of BCS

superconductors, which show such a dip. The DOS there is fitted well with the BCS theory, and the inferred gap $\Delta(T)$ vanishes at T_c). It continues to temperatures much higher than T_c ; here one can see such a feature till about 166K, which is close to T^* at this doping. Another peculiar observed feature is that the peak to peak energy (akin to $2\Delta(T)$) is roughly the same over this range of temperatures. The presence of T^* and of the pseudogap is confirmed by a very large number of measurements (see ref. [23] for a relatively recent review) such as ARPES, single particle tunnelling, NMR (magnetic susceptibility), resistivity, neutron scattering, ultrasound propagation, Kerr effect... . The range of values of T^* and the general trend as a function of x are the same; the actual numbers can and do vary.

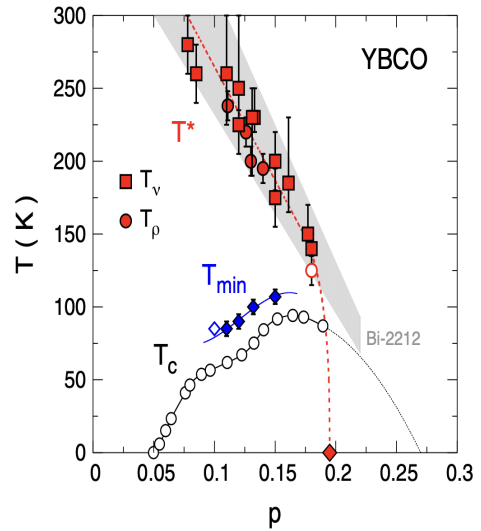


Figure 8. The pseudogap temperature $T^*(x)$ as a crossover, from transport measurements on hole doped YBCO (from Cyr-Choiniere et al., ref. [24]).

Fig. 8 from an article by O. Cyr-Choiniere et al. [24] is an example. The T^* line marking the end of the pseudogap is inferred here for hole doped YBCO from features in the Nernst effect and in the resistivity. There is a contrary view that T^* marks a line of phase transitions rather than a crossover; as evidence for it, for the same YBCO system, neutron scattering (occurrence of a new magnetic phase) data points and two points from a kink in ultrasound velocity are shown in Fig. 9 from a paper by Shekhter et al. [25].

The same figure also shows the onset of Kerr rotation, which occurs at a distinctly lower temperature, and is more compatible with the idea of a crossover. The controversy is unresolved.

Two widely prevalent conventional views about the pseudogap state are that it is either a state with

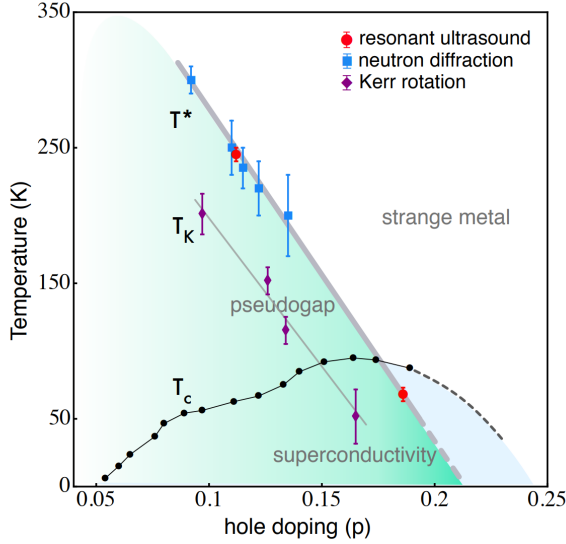


Figure 9. The pseudogap temperature $T^*(x)$ as line of phase transitions; hole doped *YBCO* (from Shekhter et al., [25]).

performed Cooper pairs, namely with Cooper pairs which are present but not phase coherent, or that it is a state with competing orders, i.e. that other kinds of electronic correlations compete with superconductive ordering tendency. There are indeed several such correlations such as stripes, charge density wave order, spin order, electronic nematic. . . .

4. Strange metal:resistance and magnetoresistance

The metallic state beyond the pseudogap line (generally with doping $x > x_{opt}$), quite actively investigated recently, is strange. It does not seem to have well defined electronic quasiparticles. The dc electrical resistivity and magnetoresistance are linear in temperature and magnetic field respectively. We discuss this state now.

A figure from a recent article by Phillips, Hussey and Abbamonte [26] entitled ‘stranger than metals’ highlights the electrical resistivity. It shows the resistivity of slightly overdoped *LSCO*, with $x = 0.21$. It increases linearly with temperature from $T_c (\approx 30K)$ to the highest accessible temperature (in this case about $500K$). ¶ There are no signs of its bending over, namely of resistivity saturation (which is a common but not well understood phenomenon in many highly resistive clean metals, see e.g. ref. [27]). The resistivity goes right through the quantum limiting value, called the Mott Ioffe Regel or MIR limit (in

¶ Linear resistivity has been recognized for long as a basic pointer towards a possibly new kind of quantum electronic state, e.g. by Anderson (1987) (Baskaran, private communication).

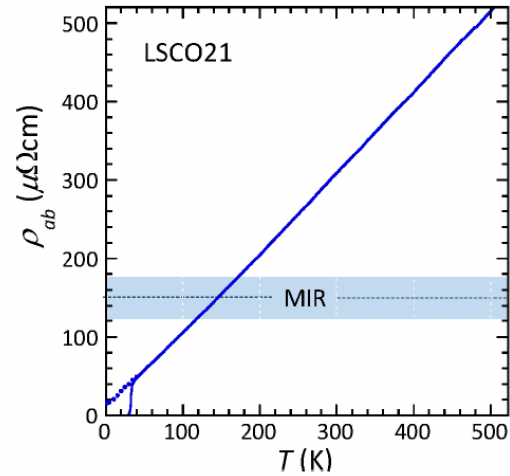


Figure 10. Electrical resistivity of $La_{2-x}Sr_xCuO_4$ for $x = 0.21$, *ab* plane as a function of T (from Phillips, Hussey and Abbamonte, [26]).

this case, estimated to be about $150\mu\Omega cm$) and can be much larger than it. + The resistivity below T_c is obtained by destroying superconductivity with a large enough magnetic field B applied perpendicular to the *ab* plane, and extrapolating the observed resistivity $\rho(T, B)$ to that for $B = 0$ (this is most commonly done by successfully fitting the measured $\rho(T, B)$ to an empirical formula and taking B to zero in it). The quantity $\rho(T, 0)$ is shown as a set of blue dots. We see that that the blue dotted line is linear in T and has the same slope. Thus, virtually from $T = 0$ to the highest temperature, the electrical resistivity is linear.

To ‘set the stage’, we show in Fig. 11 the resistivity of some metallic elements as a function of temperature. The resistivity is due to the scattering of electrons by lattice vibrations which have a characteristic quantum scale, namely the Debye temperature θ_D (symbolized by θ here). The dimensionless resistivity ($\rho(T)/\rho(\theta)$) is plotted as a function of temperature T in units of θ , namely (T/θ) , and is seen to be nearly identical for all of them, though θ varies from $175K$ to $470K$. The well known Bloch-Grueneisen formula for electron phonon resistivity (full line) fits them. We notice that for $T < 0.25\theta$, the resistivity is sublinear because of quantum effects;

+ The quantum limit is estimated via the minimum mean free path condition for resistive scattering of an electron at the Fermi energy. The Mott limit corresponds to assuming that it is equal to the quantum or de Broglie wavelength of that electron, and the Ioffe-Regel limit to taking it to be the average interatomic spacing. For typical metallic electron densities, the values for either limit are quite close to each other, and lead to numbers in the range of $150 - 400\mu\Omega cm$.

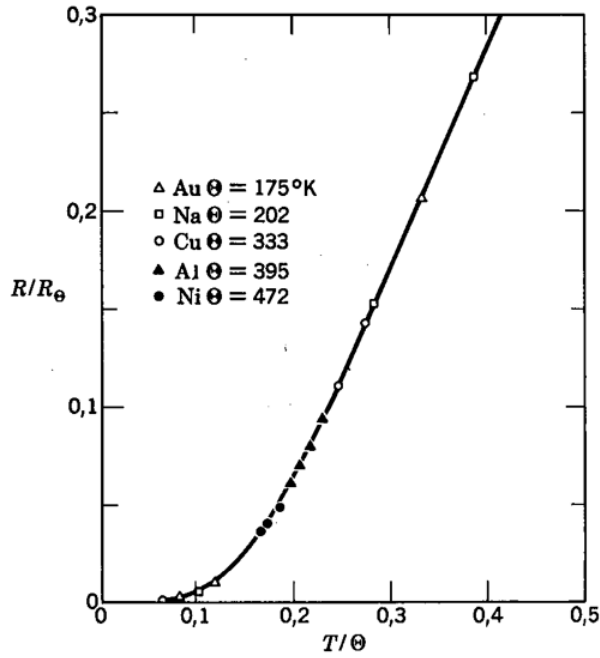


Figure 11. Electrical resistivity of some clean metallic elements as a function of T .

it is linear for higher temperatures. By contrast, the resistivity of cuprates is linear from the lowest temperatures.

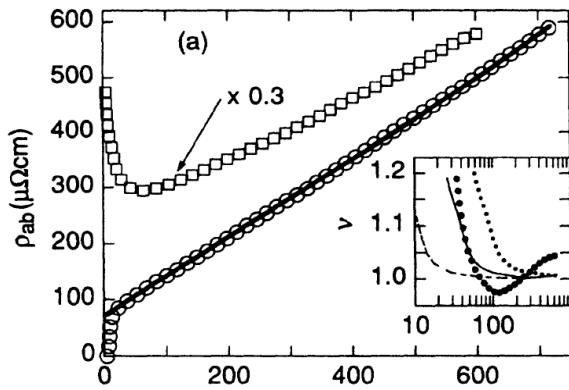


Figure 12. Electrical resistivity of a single crystalline flake of $Bi-2201$, ab plane (from Martin et al., ref. [28]).

An early result for the ab plane resistivity of single crystalline flakes of $Bi-2201$, due to Martin et al. [28] which revealed this is shown in Fig. 12. They observed the resistivity to be linear in T from T_c ($\approx 7K$) to $700K$. Attempts to fit the observation to the Bloch Grueneisen formula are shown in the inset; the set of full black dots is the observed resistivity (actually what is shown is $\nu(T)$ assuming that ρ varies as T^ν at

any particular temperature T). None of the curves with various presumed Debye temperatures varying from $10K$ to $80K$ fits the data well, even though these are unacceptably low values since the thermodynamic Debye temperature is expected to be $350K$. Another early result, the resistivity of $LSCO$ for a huge range of hole doping levels from $x = 0.1$ to $x = 0.34$, namely underdoped to highly overdoped, is shown in Fig. 13 (from ref. [29]).

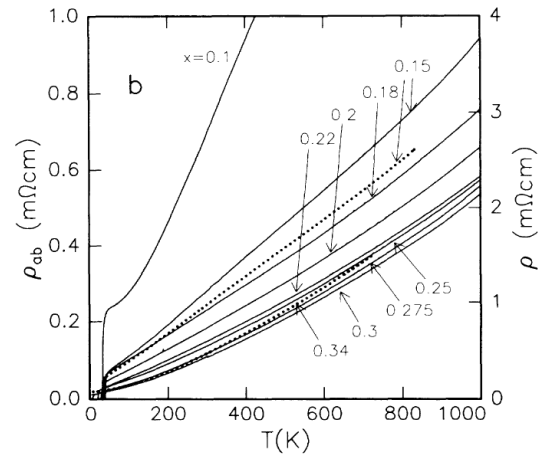


Figure 13. Electrical resistivity of hole doped $LSCO$ for a wide range of hole doping and temperature (from Takagi et al., ref. [29])

The MIR limit is about $0.4m\Omega cm$. We see very nearly linear resistivity over this entire doping range, upto high temperatures of order $1000K$, with values well above the MIR limit. In twisted bilayer graphene, for example, the effective upper temperature can be extended by orders of magnitude; the resistivity is seen to continue being linear. This is achieved in twisted bilayer graphene (TBG) for angles near the magic angle of 1.1° , for which the tight binding graphene band is flat ($t_{eff} = 0$) as follows. The bandwidth is specially small close to this twist angle, on both sides of it. The local electron repulsion is not affected seriously by small changes in the twist angle between the bilayer constituents, so that one will inevitably have $(U/t_{eff}) \gg 1$ or effectively strong correlation very close to the magic angle; the ratio obviously decreases as one moves away from the magic angle (and t_{eff} increases). If linear resistivity is a characteristic feature, not just of cuprates, but of all strongly correlated systems, one expects linear resistivity near the magic angle in TBG as well. Further, because of the small carrier density in these systems (typically, $n_h \approx 10^{12}/cm^2$) the effective Fermi energy ϵ_F^* is small $\approx 30-35K$ and one can investigate the resistivity upto temperatures of the order of ϵ_F^* . The resistivity of TBG at different angles of twist and temperatures is shown in Fig. 14 ref. [30]. We see that a nearly linear

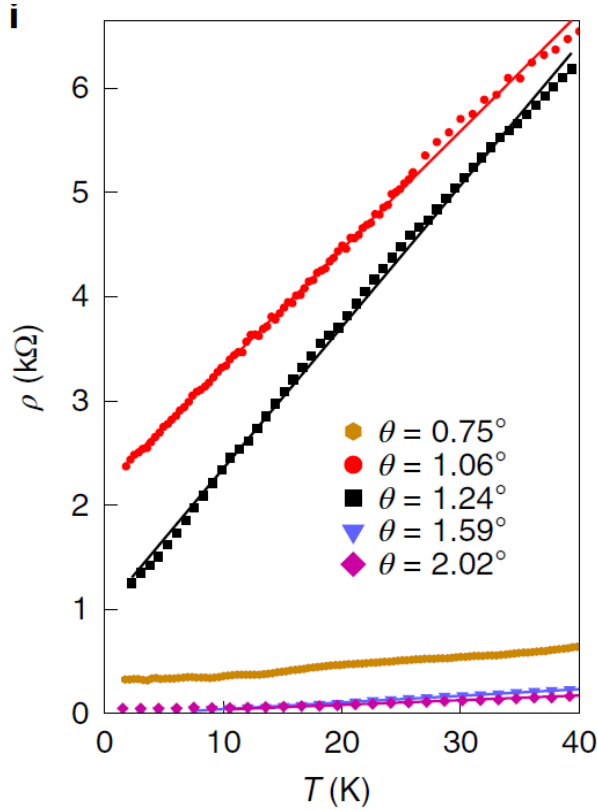


Figure 14. Electrical resistivity (resistance per square) of twisted bilayer graphene for different twist angles near the magic twist angle (from Polshyn et al., ref. [30]).

temperature dependence of resistance continues upto temperatures as high as ε_F^* . (In the cuprate language, we can access temperatures as high as $\sim 20K$!).

Things have got curioiser in the last few years, with high quality measurements and analyses of $\rho(B, T)$ for clean, well characterized, mostly overdoped, cuprates ; the external field B ranges here upto $\approx 60T$. The overdoped regime is preferred because the complexities of pseudogap and other possible competing order such as charge order (CDW?) are absent there. Further, since T_c is small, it is possible to destroy superconductivity with large but accessible magnetic fields.

An example of the results is shown in Fig. 15 taken from the paper of Legros et al. [31]. The magnetic field dependent part of $\rho(B, T)$ is seen to go as B^2 for different small values of B . This enables one to extrapolate to $\rho(0, T)$. Because the measurements are made in high fields, one can access the regime $T < T_c$, and find $\rho(0, T)$ for $T < T_c$. Some results for overdoped $Bi - 2212$ ($x = 0.23$) are shown in the figure. We see that the data fall on the linear resistivity curve for $T > T_c$ extrapolated to values below T_c ; the resistivity slopes are the same. This is quite remarkable, also because it is a physical property

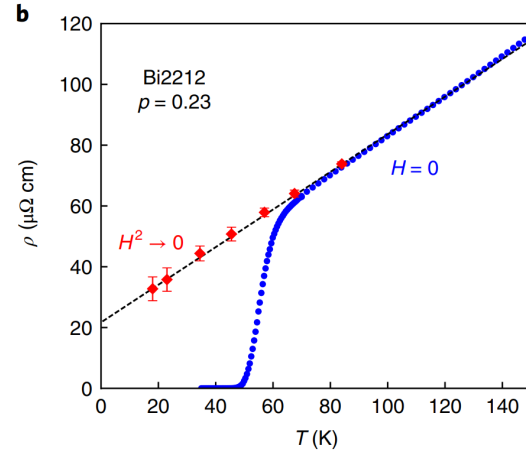


Figure 15. Electrical resistivity of overdoped $Bi - 2212$ ($p = 0.23$), extrapolated to $B^2 = 0$ (from Legros et al., ref. [31]).

of a thermodynamically unstable state (the stable state below T_c , at $B = 0$, is of course superconducting with $\rho(T) = 0$!). Even more interestingly, the magnetoresistance at high fields is observed to be linear in B . This is seen from Fig. 16. (Ayres et al., ref. [32]) which shows measurements on overdoped $Tl - 2201$ (with $x \approx 0.27$ and $T_c \approx 26.5K$).

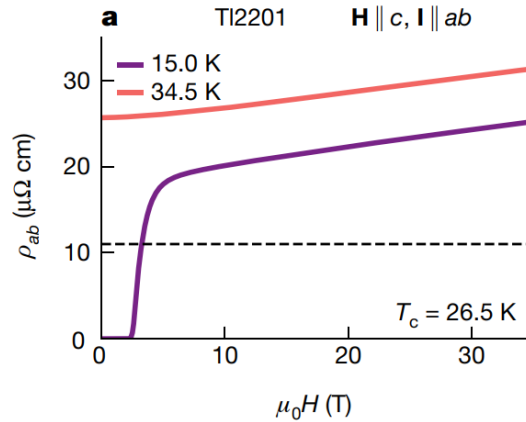


Figure 16. Linear magnetoresistance in overdoped $Tl2201$ ($p = 0.27$) (from Ayres et al., ref. [32]).

This is surprising since so long as $\mu_B B \ll \varepsilon_F$ or $\mu_B B \ll \hbar/\tau$, which is generally the case in metals, the magnetoresistance goes as B^2 . Here however, the magnetoresistance starts as B^2 for low fields and becomes proportional to B for high fields such that $\mu_B B > k_B T$. The slope of the magnetoresistance is seen to be independent of T . The empirical relation $\rho(B, T) = F(T) + \sqrt{(aT)^2 + (bB)^2}$ is found to fit the data well. (This form has of course the observed low and high B behaviour). Even

more intriguing is the recent finding that in energy units, the slope of the linear resistivity and of the linear magnetoresistance are the same for the three overdoped cuprates investigated (ref. [33], Fig. 17).

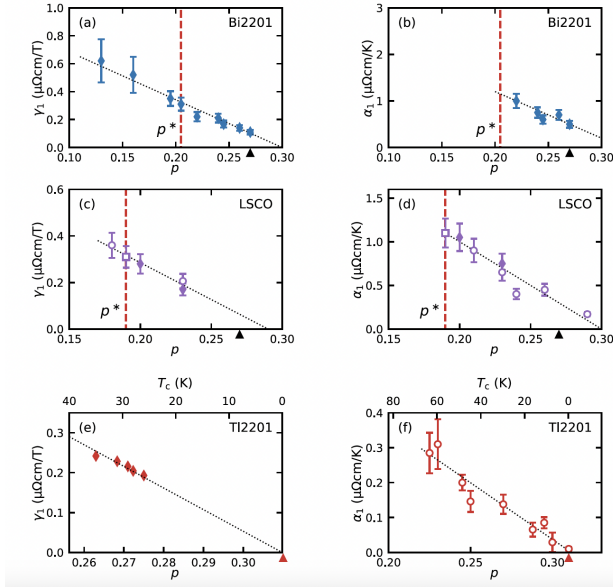


Figure 17. Comparison of slopes of linear resistivity and linear magnetoresistance in three overdoped cuprates (from Ayres et al., ref. [33]).

5. Empirical correlations

We present below some empirically observed correlations between two experimentally measured cuprate superconductor quantities. Perhaps the oldest such correlation, due to Uemura (1989), is between two equilibrium properties of the superconductor, namely between T_c and superfluid density or more accurately T_c and $(1/\lambda^2)$ where λ is the London or magnetic penetration depth.* A figure from a more recent paper [34] by Uemura (Fig. 18 shows a broad correlation for a number of cuprates (generally in the underdoped regime) and other systems. The correlation is not restricted to underdoped cuprates; for example, it is observed in well characterized overdoped *LSCO* films with x ranging from about 0.17 to 0.27. Here, the absolute value of $1/\lambda^2$ was measured accurately by a mutual inductance method. The connected superfluid stiffness $N_{so}(= A/\lambda^2)$ where A involves only universal constants) displayed against T_c [35] (Fig. 19).

A clear linearity is evident. Very near the *QCP*

* Uemura measured the width σ of the Gaussian spread in the Larmor precession frequencies of decaying spin polarized muons injected into the cuprate superconductor. A magnetic field is applied perpendicular to the *ab* plane. He found that the width is proportional to T_c , with a universal slope. One can show fairly generally that $\sigma \propto 1/\lambda^2$, so that one has $T_c \propto 1/\lambda^2$.

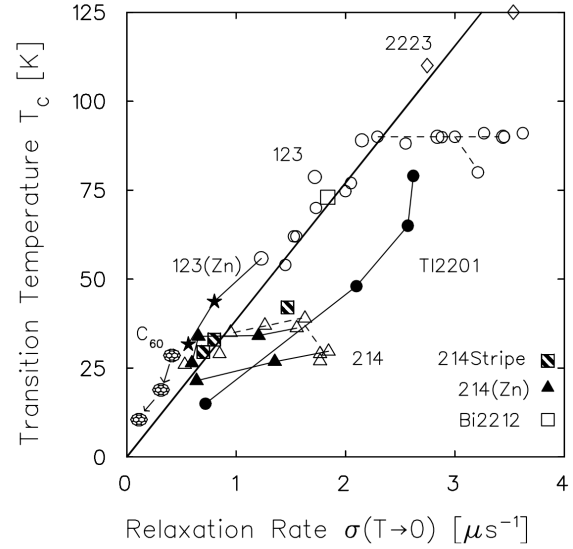


Figure 18. Uemura correlation between T_c and superfluid density (measured here via muon spin relaxation) (from Uemura, ref. [34]).

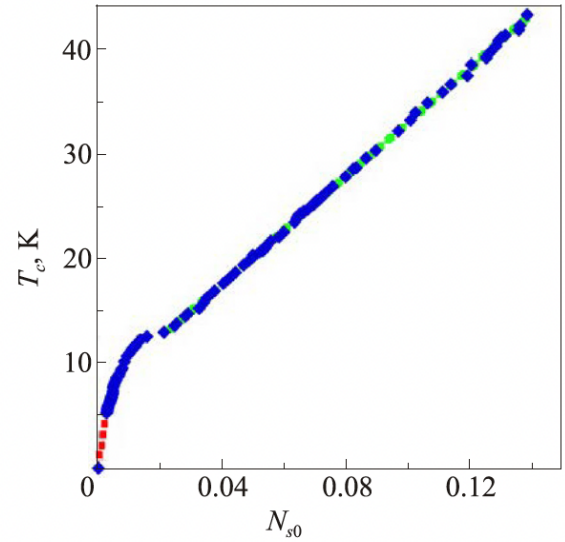


Figure 19. Correlation between T_c and superfluid stiffness in overdoped *LSCO* (from Bozovic et al., ref. [35]).

where $T_c \rightarrow 0$, the quantum critical behaviour $\sqrt{N_{so}} \propto T_c$ is observed. A peculiar common feature of the superconducting state ($T \ll T_c$), perhaps related to this, is that $N_s \propto T$ over a wide range of temperatures except for very low ones, where it goes as T^2 .

An older empirical correlation is between (t'/t) and $T_{c,max}$ due to Pavarini et al. [36]. An effective one band model for a stoichiometric cuprate family member was obtained by starting with a large number of possibly relevant states and integrating out states

other than those corresponding to the tight binding local $d_{x^2-y^2}$ symmetry band. The 'renormalized' parameters of the effective one band model were determined. It was noticed, surprisingly, that (t'/t) (obtained for the undoped cuprate) is proportional to the maximum value of T_c of the hole doped cuprate. A purely experimental version of this correlation, for the actual hole doped cuprate is due to W. S. Lee et al. [37]. They determined the location of the Fermi surface of the metal with $T_{c,max}$ from ARPES and fitted it with tight binding parameters. Their plot of $T_{c,max}$ vs. (t'/t) (inferred at x_{opt}) is shown in Fig. 20.

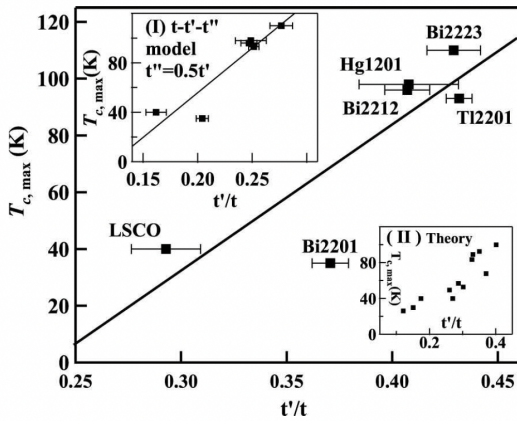


Figure 20. Correlation between the maximum T_c of a cuprate, namely $T_{c,max}$ and next nearest neighbour hopping t' (in units of nearest neighbour hopping t) (from Lee et al. ref. [37]).

This is surprising, because the superexchange term $J\mathbf{S}_i \cdot \mathbf{S}_j$ where $J \approx (t^2/U)$ can also be thought of as the nearest neighbour (intersite) Cooper pairing term in the Hamiltonian; one therefore expects a linear relation between T_c and t^2 , not between T_c and t' . Support for t' being relevant comes also from huge enhancement of d wave superconducting correlations (observed via ac conductivity measurements) due to resonant laser excitation of the apical oxygen vibrational mode. (Ref. [38], Fig. 21)

One can interpret this as follows. The next nearest neighbour hopping amplitude t' has a large contribution from the overlap between the p orbital of the apical oxygen with $d_{x^2-y^2}$ symmetry orbital at sites i . One therefore has a term in t' which is of the second order in the overlap t_{pd} . The pd overlap and so t_{pd} can be increased by resonant excitation, increasing t' and thus d wave superconducting correlations in the spirit of this empirical finding.

Another interesting correlation is between a sharp peak observed in the inelastic scattering of neutrons from the cuprate superconductor for $\mathbf{Q} = (\pi/a, \pi/b)$ and T_c . The peak is quite sharp below T_c . (This is known as the '41meV' resonance for historical reasons).

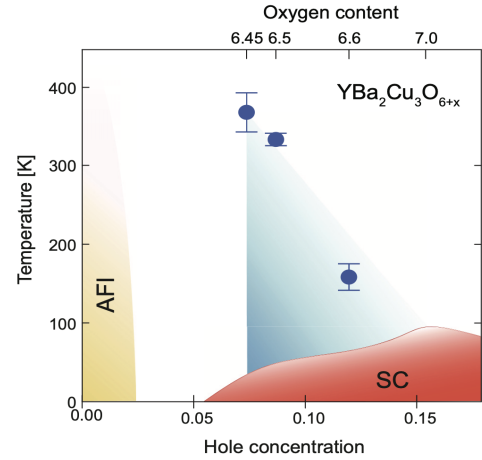


Figure 21. Correlation between nonequilibrium superconducting phase generated by resonant laser excitation of apical oxygen vibrational mode and hole density in $YBCO$, in the temperature (T) hole density (x or p) plane (from Kaiser et al. ref. [38]).

The resonance energy E_r is proportional to T_c in a number of cuprates, with a proportionality constant close to 6. The T_c values range from about 25K to about 100K (see Fig. 21). Finally, we mention a characteristic effect in cuprates connected with a nondissipative transport property, namely the Hall effect. It has attracted a lot of attention recently and is the crossover in the inverse Hall number from p (hole doping) to $(1+p)$ as p goes highly overdoped. This is shown in Fig. 22 which is reproduced from a paper by C.Putzke et al. [39].

We see a fairly large crossover region (from $p \approx 0.17$ to $p \approx 0.27$) over which this happens, in a number of overdoped cuprates. As in the standard Hall configuration, the Hall strip is in the xy plane (ab plane of the cuprate). An electric field E_x is applied in the x direction as a consequence of which there is an electric current in that direction with current density j_x . A magnetic field B_z is applied perpendicular to the xy plane (along the c -axis, in our case). A Hall electric field E_y develops in the y direction. The Hall number $R_H = (E_y/j_x B_z)$ and can be used to define (experimentally) a 'carrier density' n_H as $R_H = (1/n_H e)$. In most metals and semiconductors, this is indeed seen to be the density of electron or hole current carriers. In cuprates, this number depends significantly on a temperature scale of order 100K, much smaller than an electronic scale, so that its identification with carrier density is not convincing. At low temperatures and at high magnetic fields, the experimentally observed ratio R_H rises from zero in the superconducting state and becomes field independent as well as nonzero when superconductivity is destroyed. The inverse of this number (in units of e), namely n_H is seen for $x < 0.16$ to be

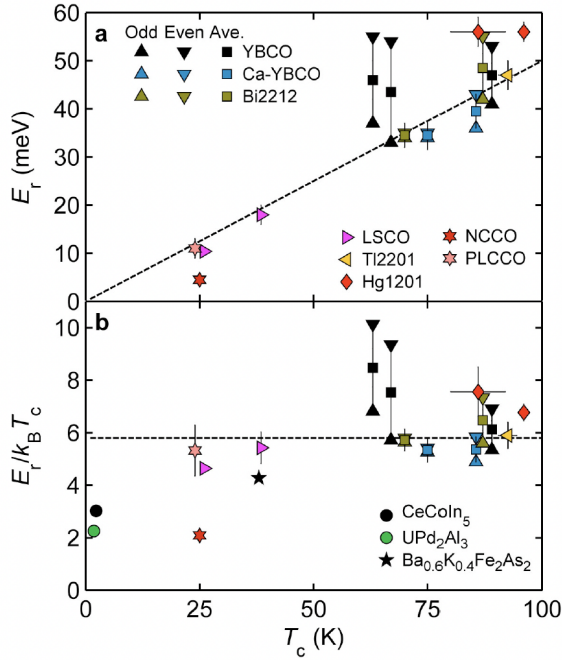


Figure 22. Correlation between neutron resonance (‘41meV resonance’) energy and T_c (from Yu et al. ref. [40]).

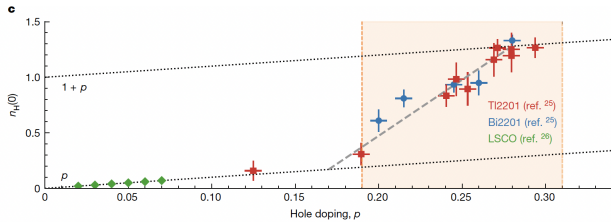


Figure 23. Inverse Hall number as a function of hole doping, specially the crossover for overdoping (from Putzke et al. ref. [39]).

the hole density x (it is called p in the figure). \ddagger The finding is that as x increases from mildly overdoped ($x > 0.17 - 0.18$) to highly overdoped ($x \approx 0.27$), n_H increases from x to $(1 + x)$.

We conclude by mentioning an unexpected relation between the strange metal above T_c and superconductivity. The measured linear resistivity of the strange metal has a slope A which is correlated with T_c in a variety of systems. This has been known for some time (e.g. the review by L. Taillefer [41] in 2010 entitled ‘Scattering and Pairing in Cuprate Superconductors’).

\ddagger The number of mobile electrons per unit cell is $(1 - x)$ for x holes per unit cell. The total number of electron states in the Brillouin zone is two per unit cell; for $(1 - x)$ electrons in this BZ (occupying $(1 - x)$ of those states), the number of unoccupied or hole states is $(1 + x)$.

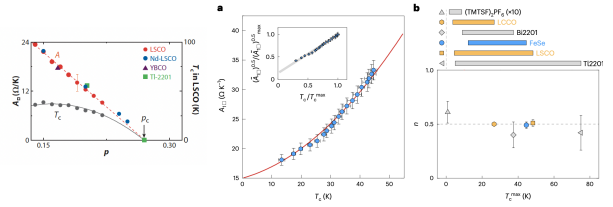


Figure 24. Correlation between slope A of the linear resistivity and T_c ($A^{0.5} \propto T_c$) (from Jiang et al. ref. [42]).

More precisely, we see in Fig. 24 that in many compounds (not only cuprates), $A^{0.5} \propto T_c$. The correlation was first brought out [42] in extensive work on *FeSe*, whose T_c can be tuned from 13K to 45K, and was generalized to show that it holds for cuprates and organics in addition as is shown in Fig. 3 of that reference. An interesting aspect of this correlation is that a thermodynamic equilibrium property connected with pairing coherence, namely T_c , is related to the nonequilibrium property of electrical current, namely to electrical resistivity (which arises from incoherent or dissipative scattering). $\rho = AT$.

6. Trying to make sense of the goings on

We notice that broadly, two kinds of strange properties of cuprates have been described above. One is related to their superconductivity i.e. to nonzero T_c , for example the correlation between (t'/t) and T_c . The other kind of behavior, e.g. linear resistivity, does not involve T_c or superconductivity per se. The two seem connected, at least in the cuprates; for example, the slope A of the linear resistivity is connected with T_c ; specifically we have $\sqrt{A} \propto T_c$. The large amount of related activity generated is not discussed here; there is an overarching idea that these materials are strongly correlated, and that this is the key to all their properties including their superconductivity. If the system is very strongly correlated so that doubly occupied on site states are projected out (as is identically true for $U = \infty$), the nonsuperconducting state is a projected Fermi liquid. The idea goes back to Gutzwiller in 1963 (see for example ref.44 for a relatively recent summary) and was explored also in conjunction with the RVB mechanism of superconductivity. Its implementation over a range of correlation strengths (and ranges), doping ranges, temperatures, dimensions, lattice types etc. is an ongoing activity. As mentioned earlier, the basic ingredient of superconductivity in the strong correlation RVB approach of Anderson, Baskaran is the nearest neighbour superexchange J , a ‘small’ quantity $\sim (t^2/U) = t(t/U) \ll t$.

In this spirit, one should perhaps look for a new picture for many electron systems founded explicitly

on the $U = \infty$ limit and build from there (for example a theory in the small parameter $(t/U) \sim (0.1) \ll 1$ in the cuprates) in the hope of a comprehensive understanding of this collection of strange properties. For many electron systems in a lattice model, this can be motivated by the fact that there are two obvious limits, namely one of $U = 0$ and the other of $U = \infty$. The first is exactly soluble analytically for the continuum case and is described by the Drude free electron gas theory. †† For nonzero interaction (nonzero U), there are very sophisticated and highly developed theories which are finally perturbative in U ; they are adiabatically connected to the no interaction limit. Our efforts so far to understand the cuprates are generally rooted in this limit (often with additional auxiliary fields and constraints). The other limit is the metallic state for infinitely strong correlations ($U = \infty$). The many electron problem is not exactly soluble in this limit and there are very few theoretical methods available for exploring it. We need reliable (necessarily approximate) solutions to answer the question: does it qualitatively describe strongly correlated metals and their superconductivity?

In this light, before mentioning our results for a paradigmatic approach to the $U = \infty$ limit I present a piece of experimental evidence which suggests that at least in hole doped cuprates the electron correlation U continues to be both large and nearly unchanged for hole doping p ranging from 0 (undoped) to 0.27 (overdoped), so that this limit small (in $(1/U)$ departures from $U = \infty$ are relevant. The evidence is the (broadened) spin wave spectrum of doped cuprates obtained via inelastic neutron scattering studied using RIXS, the excitation energies being as large as 200 meV. It is found that for large values of \mathbf{Q} the dispersion is unchanged for different values of doping, and is fairly accurately given by the spin wave dispersion from the nearest neighbour Heisenberg model with a J of about $1400K$. This implies strong coupling because the idea of a J meaningful only for large U , and also implies that U remains large at short distances since $J(\approx t^2/U)$ is relatively unchanged. An independent confirmation is from the nearly unchanged frequency integrated intensity of the spin wave spectrum plotted for a particular large value of \mathbf{Q} , namely $\mathbf{Q} = 0.8(\pi, 0)$, for different cuprates with hole doping ranging from 0 to 0.27 (Fig. 25).

The exploration of the metal for $U = \infty$ has been pioneered by Shastry [44] starting from 2010 and continuing, and investigated most thoroughly him. Shastry (who has named this limit as that of the Extremely Correlated Fermi Liquid or ECFL) uses

††As is well known, independent electrons in a periodic lattice or Bloch electrons are not an exactly soluble system, but are computationally accessible. They also have novel topological properties.

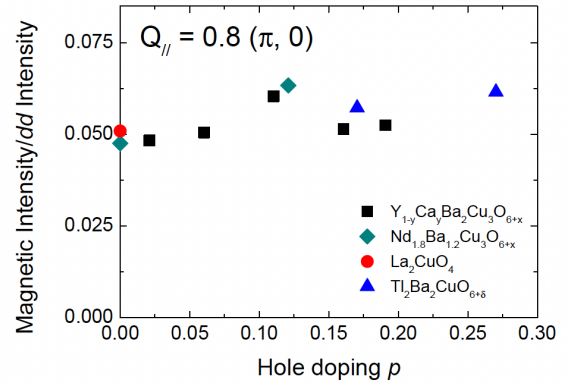


Figure 25. Energy-integrated intensity of magnetic excitations (mostly from RIXS, normalized to the dd excitation intensity) as a function of doping, for several cuprates. (from Le Tacon et al. ref. [43]).

the field source method of Schwinger, has developed a detailed systematic theoretical structure, and has applied the results to cuprates (with nonzero J where necessary). In recent work, we [45] have used an equation of motion method which we describe briefly below.

The infinitely correlated metal is faithfully described in terms of three quantum states $|ia\rangle$ at each site, namely $|i0\rangle$, $|i\uparrow\rangle$; $|i\downarrow\rangle$ or states with no particle or with one particle having spin up or down respectively. The state with two electrons at a site is infinitely high in energy and need not be included. The matrix elements in this space of states are the Hubbard operators X_i^{ab} , fermionic when a and b differ by an electron, and bosonic when a and b differ by none. They are not canonical Fermi and Bose operators since the (anti)commutators are not c numbers, but (X) operators. The Hamiltonian in this space of states is

$$H = \sum_{i,\sigma} (-\mu X_i^{\sigma\sigma}) + \sum_{ij,\sigma} t_{ij} X_i^{\sigma 0} X_j^{0\sigma}. \quad (2)$$

This would have been exactly soluble if $X_i^{\sigma 0}$ were a canonical fermion creation operator $a_{i\sigma}^\dagger$.

In the ECFL, the dynamics of the electron correlator of the type $\langle X_i^{\sigma 0}(t) X_i^{0\sigma}(t') \rangle$ involves (e.g. via the equation of motion) mixed fermionic and bosonic fluctuation correlation functions which can be decoupled in the $d = \infty$ limit. The propagation of the resulting bosonic fluctuations (charge and spin correlators) depend on electron correlators. We therefore calculate XX correlation functions self consistently. For example, spectrum of local self generated bosonic fluctuations obtained this way is

shown in Fig. 26. The diffusive, overdamped form, roughly characterized by a damping or width but with a long tail and characteristic broadening with temperature is evident. These fluctuations are strongly coupled to the electron dynamics, e.g. to the self energy Σ . It is seen from exact properties of spectral functions at low energies that $\text{Im}\Sigma(\omega, T)$ necessarily has the coherent liquid form $(\omega^2 + \pi^2 T^2)$ at very low frequencies ω and temperatures T . This crosses over at very low temperatures $T \approx 0.003t$ to an incoherent Fermi liquid regime. In measurable quantities like resistivity, there is a deviation towards linearity from a T^2 behaviour starting from this temperature, as seen in Fig. 27.

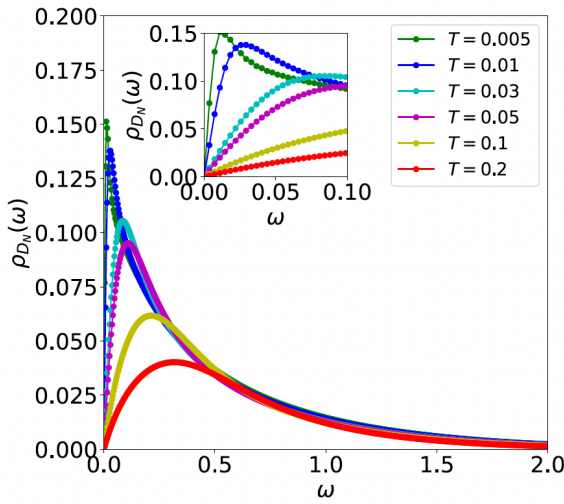


Figure 26. Normalized spectral density $\rho_{DN}(\omega)$ of local bosonic fluctuations for hole doping $x = 0.3$ as a function of frequency ω for various temperatures T (in units of the nearest neighbour hopping t) (from Hassan et al. ref. [45]).

This figure also shows the ubiquitous linear resistivity behaviour with the low crossover temperature for it, clearly apparent in the inset. On a larger temperature scale, the linear behaviour seems to be composed of two linear segments with a crossover. Other indications, e.g. from $\text{Im}\Sigma(0, T)$ and single particle spectral density, also support this crossover to an incoherent Fermi liquid (which has linear resistivity). This seems to be a paradigmatic behaviour associated with strong correlation. In terms of the bosonic fluctuations, this is brought out in Fig. 28 where I plot the average energy $\Omega = \langle \omega \rangle$ of the bosonic fluctuation against temperature.

One sees clearly the coherent Fermi liquid regime at very low temperatures. There is a ‘classical’ regime for which $T > \Omega$. In between, there is a large incoherent Fermi liquid regime, which is dominated by local quantum bosonic fluctuations. In this regime the

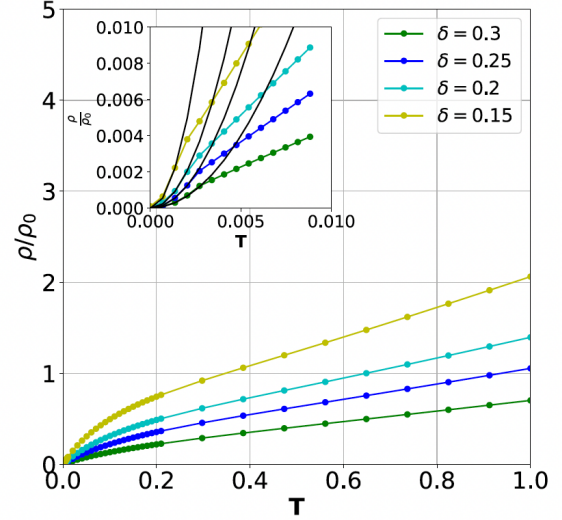


Figure 27. Electrical resistivity as a function of temperature, for different values of doping (from Hassan et al., ref. [45]).

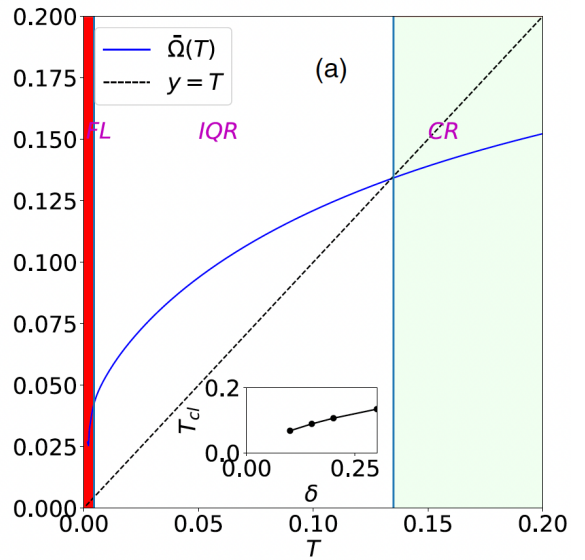


Figure 28. Average bosonic fluctuation energy $\Omega(T) = \langle \omega \rangle$; (in units of t) as a function of temperature (in units of t) for doping $x = 0.3$. The coherent Fermi liquid (FL), incoherent quantum regime (IQR), and the classical regime (CR) are also shown (from Hassan et al., ref. [45]).

thermal energy is small compared to the average energy of diffusive fluctuations which can also be thought of as quantum electrical noise at each lattice site (‘white’ in the sense that the strength does not depend on the frequency). We believe that we have unearthed two crucial features of ECFL: one is that there are strong, local, diffusive, self generated, bosonic (charge and spin) fluctuations coupled to electrons and the other is that there is, consequently, a large incoherent quantum

regime.

However, while it seems plausible that some unusual properties of the metallic state (e.g. the incoherent Fermi liquid state and ubiquitous linear resistivity) are paradigmatic features of strong correlations and are captured in a $U = \infty$ theory, we cannot and do not compare its results with real systems yet for several reasons, some of which are the following. The theory is still too opaque, technically weak, and complicated; it needs to be perhaps cast in a different, more accessible form which explicitly brings out our observations and results. We have worked with a paramagnetic state, while the ground state is believed to be a (Nagaoka) ferromagnet at least for quite low hole densities so that for such densities one is starting with the ‘wrong’ ground state. The crossover from a coherent to an incoherent Fermi liquid occurs at a very low temperature the origin of whose small scale is not clear. Real strongly correlated systems have a large but finite U , so that there must be significant ($1/U$) effects (including d -wave superconductivity and many of the phenomena described above). Maybe with a theory which includes $O(1/U)$ effects one can confront experiments. Such a ($1/U$) perturbation theory is being developed.

To conclude, we have been faced with a strange beast called Cuprate High Temperature Superconductors for many decades (and now, we have many like them). We know many of its characteristics; some have been described above. We have been trying (not quite successfully) to describe them in the language we know. Maybe a different language is needed.

7. Acknowledgements

I am very thankful to Professor Tanusri Saha-Dasgupta for the opportunity to present this review like talk at the Bose centenary conference. I am also thankful to Dr. Arijit Haldar and Ms. Monalisa Chatterjee for help with the typescript.

References

- [1] Bose S N 1924 *Zeit. für Physik* **26** 178 URL <https://doi.org/10.1007/BF01341708>
- [2] Einstein A 1924 *Preuss. Akad. Wiss* **261** 1924
- [3] London F 1938 *Nature* **141** 643–644
- [4] London F 1948 *Physical Review* **74** 562
- [5] London F 1950 “*Superfluids: Macroscopic theory of superconductivity*” (Wiley, New York)
- [6] Bardeen J, Cooper L N and Schrieffer J R 1957 *Phys. Rev.* **108** 1175
- [7] Sheshadri K, Malterre D, Fujimori A and Chainani A 2023 *Phys. Rev. B* **107** 085125
- [8] Bednorz J G and Müller K A 1986 *Zeitschrift für Physik B Condensed Matter* **64** 189–193
- [9] Anderson P W 1987 *Science* **235** 1196–1198
- [10] Klitzing K v, Dorda G and Pepper M 1980 *Phys. Rev. Lett.* **45** 494
- [11] Keimer B, Kivelson S A, Norman M R, Uchida S and Zaanen J 2015 *Nature* **518** 179–186
- [12] Schrieffer J R 2007 “*Handbook of High -Temperature Superconductivity: Theory and Experiment*” (Springer)
- [13] Ganguly P and Rao C N R 1984 *J. Solid State Chem.* **53** 193
- [14] Presland M, Tallon J, Buckley R, Liu R and Flower N 1991 *Physica C: Superconductivity* **176** 95–105
- [15] Zaanen J, Sawatzky G and Allen J 1985 *Phys. Rev. Lett.* **55** 418
- [16] Zhang F and Rice T 1988 *Phys. Rev. B* **37** 3759
- [17] Ogata M and Fukuyama H 2008 *Rep. Prog. Phys.* **71** 036501
- [18] Baskaran G, Zou Z and Anderson P 1987 *Solid State Commun.* **63** 973–976 ISSN 0038-1098
- [19] Anderson P W, Lee P, Randeria M, Rice T, Trivedi N and Zhang F 2004 *J. Condens. Matter Phys.* **16** R755
- [20] Norman M R 2011 *Science* **332** 196–200
- [21] Božović I, Wu J, He X and Bollinger A 2019 *Physica C: Superconductivity and its Applications* **558** 30–37
- [22] Kordyuk A 2015 *Low Temp. Phys.* **41** 239 URL <https://api.semanticscholar.org/CorpusID:56392827>
- [23] Mueller E J 2017 *Rep. Prog. Phys.* **80** 104401
- [24] Cyr-Choinière O, Daou R, Laliberté F, Collignon C, Badoux S, LeBoeuf D, Chang J, Ramshaw B, Bonn D, Hardy W et al. 2018 *Phys. Rev. B* **97** 064502
- [25] Shekhter A, Ramshaw B, Liang R, Hardy W, Bonn D, Balakirev F F, McDonald R D, Betts J B, Riggs S C and Migliori A 2013 *Nature* **498** 75–77
- [26] Phillips P W, Hussey N E and Abbamonte P 2022 *Science* **377** eabh4273
- [27] Gunnarsson O, Calandra M and Han J 2003 *Rev. Mod. Phys.* **75** 1085
- [28] Martin S, Fiory A T, Fleming R, Schneemeyer L and Waszczak J V 1990 *Phys. Rev. B* **41** 846
- [29] Takagi H, Batlogg B, Kao H, Kwo J, Cava R J, Krajewski J and Peck Jr W 1992 *Phys. Rev. Lett.* **69** 2975
- [30] Polshyn H, Yankowitz M, Chen S, Zhang Y, Watanabe K, Taniguchi T, Dean C R and Young A F 2019 *Nature Physics* **15** 1011–1016
- [31] Legros A, Benhabib S, Tabis W, Laliberté F, Dion M, Lizaire M, Vignolle B, Vignolles D, Raffy H, Li Z et al. 2019 *Nature Physics* **15** 142–147
- [32] Ayres J, Berben M, Čulo M, Hsu Y T, van Heumen E, Huang Y, Zaanen J, Kondo T, Takeuchi T, Cooper J et al. 2021 *Nature* **595** 661–666
- [33] Ayres J, Berben M and Duffy C 2024 *Nat. Commun.* **15** 8406
- [34] Uemura Y 2004 *J. Condens. Matter Phys.* **16** S4515
- [35] Božović I, He X, Wu J and Bollinger A 2016 *Nature* **536** 309–311
- [36] Pavarini E, Dasgupta I, Saha-Dasgupta T, Jepsen O and Andersen O 2001 *Phys. Rev. Lett.* **87** 047003
- [37] Lee W, Yoshida T, Meevasana W, Shen K, Lu D, Yang W, Zhou X, Zhao X, Yu G, Cho Y et al. 2006 *arXiv preprint cond-mat/0606347*
- [38] Kaiser S, Hunt C R, Nicoletti D, Hu W, Gierz I, Liu H, Le Tacon M, Loew T, Haug D, Keimer B et al. 2014 *Phys. Rev. B* **89** 184516
- [39] Putzke C, Benhabib S, Tabis W, Ayres J, Wang Z, Malone L, Licciardello S, Lu J, Kondo T, Takeuchi T et al. 2021 *Nature Physics* **17** 826–831
- [40] Yu G, Li Y, Motoyama E and Greven M 2009 *Nature Physics* **5** 873–875
- [41] Taillefer L 2010 *Annu. Rev. Condens. Matter Phys.* **1** 51–70
- [42] Jiang X, Qin M, Wei X, Xu L, Ke J, Zhu H, Zhang R, Zhao Z, Liang Q, Wei Z et al. 2023 *Nature Physics* **19** 365–371
- [43] Le Tacon M, Minola M, Peets D, Moretti Sala M, Blanco-Canosa S, Hinkov V, Liang R, Bonn D, Hardy W, Lin C et al. 2013 *Physical Review B—Condensed Matter and Materials Physics* **88** 020501

- [44] Shastry B S 2010 *Physical Review B—Condensed Matter and Materials Physics* **81** 045121
- [45] Hassan S, Prakash G, Vidhyahiraja N and Ramakrishnan T 2024 *Phys. Rev. B* **110** 075106